# Four-jet final state in same-sign lepton colliders and neutrinoless double beta decay mechanisms

C. H. Kom[1,2] and W. Rodejohann[3]

[1]*Cavendish Laboratory, University of Cambridge, CB3 0HE, United Kingdom*
[2]*Department of Applied Mathematics and Theoretical Physics, University of Cambridge, CB3 0WA, United Kingdom*
[3]*Max-Planck-Institut für Kernphysik, Postfach 103980, D-69029, Heidelberg, Germany*

(Received 20 October 2011; published 20 January 2012)

If neutrinoless double beta decay is observed, it will be important to understand the mechanism(s) behind this process. Using a minimal supersymmetric extension to the standard model in association with a lepton number violating coupling as an example, we show that if neutrinoless double beta decay is mediated by new TeV scale particles, looking for four-jet final states in future linear colliders operating in the same-sign electron mode could provide important information on the underlying mechanisms. We study the prospects for observing this process at the proposed ILC and CLIC energies, and discuss the complementarity between such a four-jet signal and other collider signatures at the LHC.

DOI: 10.1103/PhysRevD.85.015013 PACS numbers: 12.60.Jv, 13.66.Lm, 14.80.Ly

## I. INTRODUCTION

The observation of neutrinoless double beta decay ($0\nu\beta\beta$) would be an important step toward understanding the structure of physics beyond the standard model [1–3]. It would prove that lepton number, an accidental symmetry of the standard model, is violated. After establishing this, the next task would be to identify the underlying mechanism of $0\nu\beta\beta$.

The standard interpretation of $0\nu\beta\beta$ is the so-called light (Majorana neutrino) mass mechanism. In this mechanism, the $0\nu\beta\beta$ amplitude is proportional to a neutrino mass term that violates lepton number explicitly by 2 units. If this is the only source of lepton number violation (LNV) in $0\nu\beta\beta$, the rate of $0\nu\beta\beta$ can further provide information on the neutrino mass scale and ordering realized by nature, and other neutrino properties. Within the standard interpretation, $0\nu\beta\beta$ experiments become neutrino experiments.

However, if there are additional sources of LNV (nonstandard interpretations), they could dominate the amplitude when compared with contributions from the light mass mechanism. For example, $0\nu\beta\beta$ can be mediated by models with heavy Majorana neutrinos [4], Higgs triplet models [5], left-right symmetric extensions to the standard model [6], leptoquarks [7], and supersymmetric models that violate lepton number [8]. In the context of nuclear physics experiments, these possibilities are expected to be differentiated to certain extents by measuring half-life ratios of different isotopes, angular or energy correlations between the electrons from $0\nu\beta\beta$, nuclear decay to excited states, and/or electron capture. A recent review on the different proposed mechanisms and possibilities to distinguish them from each other can be found in Ref. [2].

Another approach, which we will follow here, is to search for other processes in which the underlying physics of $0\nu\beta\beta$ is present. Depending on the underlying LNV model, signatures related to $0\nu\beta\beta$ might also be observed at colliders with TeV scale collision energies. This is based on the observation that the lower limit on $0\nu\beta\beta$ half-lives, for example, that of $^{76}$Ge ($T_{1/2}(^{76}\mathrm{Ge})$) measured in the Heidelberg-Moscow experiment [9],

$$T_{1/2}(^{76}\mathrm{Ge}) \geq 1.9 \cdot 10^{25}\ \mathrm{yrs}, \tag{1}$$

corresponds generically to an amplitude with $\mathcal{O}(1\ \mathrm{TeV})$ scale and $\mathcal{O}(1)$ dimensionless LNV couplings. This is obvious from estimating the amplitude for light neutrino exchange,

$$\mathcal{A}_{\mathrm{light}\nu} \simeq G_F^2 \frac{m_{ee}}{\langle q^2 \rangle} \sim \mathrm{TeV}^{-5}, \tag{2}$$

where $G_F$ is the Fermi constant, $m_{ee}$ the effective mass set to its upper limit of order 0.5 eV, and $\langle q^2 \rangle$ the squared momentum transfer in the process, which is of order $0.01\ \mathrm{GeV}^2$.

If the TeV scale corresponds to the mass of the particles involved in $0\nu\beta\beta$, they could be produced at colliders such as the LHC and future linear colliders. If these particles are (not) observed in certain LNV signals, the information could be used to (dis-)favor particular TeV scale $0\nu\beta\beta$ models. Furthermore, studying $0\nu\beta\beta$ mechanisms through related collider processes allows direct access to the underlying physics at the particle level, separated from the notorious complication in the nuclear physics calculation, the latter of which is however necessary when computing $0\nu\beta\beta$ decay rates.

At parton level, collider processes that are the most closely related to $0\nu\beta\beta$ should violate electron number by two units, involve four first generation (initial and/or final state) quarks and no missing energy, for instance, due to the presence of neutrinos. This is because the relevant Feynman diagrams could be reinterpreted as $0\nu\beta\beta$ diagrams after appropriate crossings. A consequence is that these related processes are controlled by the same model parameters, i.e., the same particle masses and (LNV) couplings. As an example, Refs. [10,11] show that the observation of same-sign dielectron final state in

 

association with two jets at the 14 TeV LHC could lead to predictions of $0\nu\beta\beta$ half-lives, when interpreted in the context of a minimal supersymmetric extension to the standard model (MSSM) in association with a LNV coupling $\lambda'_{111}$ ($\lambda'$MSSM). Strategies to relate LHC observables to $0\nu\beta\beta$ in left-right symmetric theories have also been discussed recently [12].

In a lepton collider, the signal most directly related to $0\nu\beta\beta$ would be

$$e^-e^- \to 4j, \tag{3}$$

when all four jets are originated from first generation (anti-)quarks. This is the collider signature we shall focus on, and is called the "4j signal" in the rest of the paper. Clearly, the 4j signal has *no* irreducible standard model (SM) background, since the SM conserves lepton number. The observation of $0\nu\beta\beta$ in one or more of the many upcoming experiments (see Ref. [3] for a recent review on their status and properties) would be a strong motivation to run a linear collider in a like-sign mode. In $0\nu\beta\beta$ mechanisms involving two SM $W$ bosons, the 4j signal arises from the "inverse $0\nu\beta\beta$" [13,14], defined as

$$e^-e^- \to W^-W^-, \tag{4}$$

followed by hadronic decays of the $W$'s into first generation quarks (see Ref. [15] for a recent study of this process). Since the branching ratio of the $W$ decaying into jets is known, knowledge of the inverse $0\nu\beta\beta$ cross section allows direct inference on the $0\nu\beta\beta$ decay rate. However, in the presence of new particle(s), their branching ratio(s) into jets must also be determined. This leads us to the studying of the four-jet final states.

The difference between the inverse $0\nu\beta\beta$ followed by hadronic $W$ decays and the more general 4j process can be important, as the source of LNV can be contained in different stages of the four-jet production. For inverse $0\nu\beta\beta$, the source of LNV must be contained within the generation of the same-sign $W$ pairs. This is the case, e.g., for the light mass mechanism or the SM with the addition of heavy Majorana neutrinos. In the case of $\lambda'$MSSM, a pair of same-sign selectrons ($\tilde{e}_L$), the superpartner of a left-handed electron, can be produced via *gauge* interactions with a $t$-channel neutralino ($\tilde{\chi}^0$),

$$e^-e^- \to \tilde{e}_L^-\tilde{e}_L^-. \tag{5}$$

This can be followed by LNV decays of the selectrons into first generation quarks via the $\lambda'_{111}$ coupling, leading to the 4j signal. Note that the $\Delta L = 2$ process is mediated by two $\Delta L = 1$ vertices, and not with an explicit $\Delta L = 2$ mass term as for processes involving Majorana light or heavy neutrinos. The presence of two intermediate *on-shell* particles in the 4j signal could hence be an important clue to the underlying $0\nu\beta\beta$ mechanism. The 4j signal cross section could also be enhanced, when the 2-to-2 $\tilde{e}_L$ pair production process is followed by decay into four jets with large branching ratios due to a large $\lambda'_{111}$. This should be compared with the light and heavy mass mechanisms, for which the stringent $0\nu\beta\beta$ half-life limit implies a relatively small 4j signal rate [14,15].

In this paper, we investigate whether in the context of $\lambda'$MSSM the 4j signal might be observable in future linear colliders, assuming $0\nu\beta\beta$ is measured in the next generation of experiments. We shall study which $\tilde{\chi}^0$-$\tilde{e}_L$ mass regions future linear colliders might be particularly sensitive to, and the effect of the presence of competing $\tilde{e}_L$ decay channels, in particular, gauge decay of $\tilde{e}_L$ into an electron and $\tilde{\chi}^0$. Implications of like-sign linear collider for other (lepton number conserving) supersymmetry searches have been discussed in Refs. [16]. We note that some results in this paper may also be relevant to left-right symmetric models, or other SM extensions with TeV scale $W'$ and heavy Majorana neutrinos which play the role of the $\tilde{e}_L$ and $\tilde{\chi}^0$.

Since related collider signatures could also be expected at the LHC, we also comment on how the 4j signal might complement other $0\nu\beta\beta$ probes at the LHC.

The paper is organized as follows: in the next section, we introduce the $\lambda'$MSSM model, and discuss features that the Feynman diagrams possess which could enhance the $e^-e^- \to 4j$ signal when compared with selected models, given the current $0\nu\beta\beta$ limit. We then explore quantitatively regions of parameter space where such enhancements are significant, and how the prospect of observation could change in light of future $0\nu\beta\beta$ data, before briefly discussing the complementarity with some related LHC signals.

## II. THE $\lambda'$MSSM MODEL

The $\lambda'$MSSM model that we consider includes a (gauge invariant) LNV superpotential term,

$$\mathcal{W}_{\lambda'_{111}} = \lambda'_{111} L_1 Q_1 D_1^c, \tag{6}$$

in addition to the standard MSSM interactions that conserve $R$-parity. The $L_1$, $Q_1$, and $D_1^c$ are the first generation lepton doublet, quark doublet, and down quark singlet superfields, respectively. This and all $R$-parity conserving interactions are invariant under a discrete $\mathcal{Z}_3$ symmetry [17]. Because baryon number is not violated in $\lambda'$MSSM, the proton is stable. The Yukawa potential derived from the above LNV superpotential includes interactions for the field combinations

$$\tilde{l}_1 q_1 d_1^c, \qquad l_1 \tilde{q}_1 d_1^c, \qquad l_1 q_1 \tilde{d}_1^c, \tag{7}$$

where the fields with (without) tildes are the supersymmetric (SM) particles in self-evident notations. These interactions violate electron number by one unit, with interaction strengths proportional to the coupling $\lambda'_{111}$. Also relevant for our discussion are the neutralinos ($\tilde{\chi}^0$) and gluinos ($\tilde{g}$), which are the superpartners of the neutral (gauge) bosons and gluons, respectively. They interact with the SM particles with gauge interaction strengths.

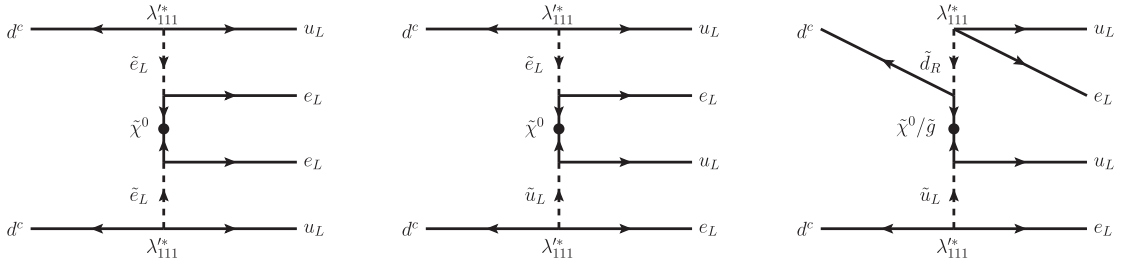


FIG. 1. Example $0\nu\beta\beta$ Feynman diagrams for $\lambda'$MSSM. The initial (final) states are on the left (right) side of the diagrams. The arrows denote the flow of left chirality, and the dots represent mass insertions in the fermion propagators required by the chiral structure. The LNV vertices are labeled with $\lambda'_{111}$.

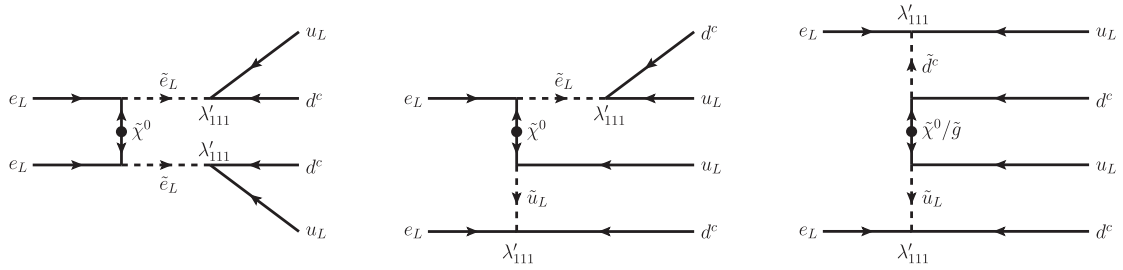


FIG. 2. Example 4j signal Feynman diagrams for $\lambda'$MSSM that correspond to the $0\nu\beta\beta$ diagrams displayed in Fig. 1. The initial (final) states are on the left (right) side of the diagrams. The arrows denote the flow of left chirality, and the dots represent mass insertions required by the chiral structure. The LNV vertices are labeled with $\lambda'_{111}$.

In Fig. 1, we show example $0\nu\beta\beta$ Feynman diagrams in $\lambda'$MSSM.[1] The corresponding Feynman diagrams for the 4j signal are displayed in Fig. 2. We see that the two sets of diagrams can be related by crossing between external legs, indicating the model parameters entering the two processes are the same. However, the 4j signal will be dominated by the diagram involving two intermediate selectrons if they can be produced *on-shell*; see the left diagram of Fig. 2. In this case the partial width and branching ratio of the selectron decaying into jets depend indirectly on the squark and gluino masses via $\lambda'_{111}$, the latter of which is extracted from an observed $0\nu\beta\beta$ half-life value. In what follows, we shall focus primarily on the case when the selectrons are produced on-shell.

Since the momentum transfer in $0\nu\beta\beta$ is much smaller than the sparticle masses involved, the effective operators for $0\nu\beta\beta$ are dimension nine operators involving six fermions. The lower $T_{1/2}(^{76}\mathrm{Ge})$ bound in Eq. (1) leads to the approximate limit [18–20]

$$|\lambda'_{111}| \lesssim 5 \cdot 10^{-4}\left(\frac{m_{\tilde{e}_L,\tilde{u}_L,\tilde{d}_R}}{100\ \mathrm{GeV}}\right)^2\left(\frac{m_{\tilde{g},\tilde{\chi}^0}}{100\ \mathrm{GeV}}\right)^{1/2}. \quad (8)$$

Actually this limit can be easily understood by comparing the standard amplitude in Eq. (2) with the expression $\mathcal{A}_{\lambda'\mathrm{MSSM}} \simeq |\lambda'_{111}|^2/(m^4_{\tilde{e}_L,\tilde{u}_L,\tilde{d}_R} m_{\tilde{g},\tilde{\chi}^0})$. While this is the most stringent single coupling bound on $\lambda'_{111}$ for sparticle masses of $\mathcal{O}(100\ \mathrm{GeV})$, it relaxes rapidly as the sparticle mass scale increases, and $\lambda'_{111}$ can be of $\mathcal{O}(1)$ if the masses involved in the dominant $0\nu\beta\beta$ diagram(s) are of $\mathcal{O}(1\ \mathrm{TeV})$.

Other single coupling bounds on $\lambda'_{111}$ come from atomic parity violation and charged current universality in the lepton and quark sectors [21]. These constraints[2] come from dimension six operators, all of which have limits of order $|\lambda'_{111}| \lesssim 0.02(m_{\tilde{d}_R,\tilde{u}_L}/100\ \mathrm{GeV})$. Because of the different mass dependence, whether the $0\nu\beta\beta$ bound is more stringent or not depends on all sparticle masses involved, and has to be calculated on a case-by-case basis.

Clearly, for the $\lambda'$MSSM all intermediate propagators can contribute to the suppression of the $0\nu\beta\beta$ rate. For comparison, in the light mass mechanism, the suppression is due to the ratio of the small mass insertion, $m_{ee} \lesssim 0.5$ eV, to the energy scale of the process $\langle q^2\rangle \simeq 0.01\ \mathrm{GeV}^2$. For the heavy neutrino mechanism, Majorana neutrinos (with mass $M_i^2 \gg \langle q^2\rangle$) which couple to the electron and $W$ boson with strength proportional to the mixing parameter $S_{ei}$ provide the mass suppression, i.e.,

$$\mathcal{A}_{\mathrm{heavy}\,\nu} \propto \frac{S_{ei}^2}{M_i}, \quad |S_{ei}| \lesssim 2.5 \cdot 10^{-3}\left(\frac{M_i}{100\,\mathrm{GeV}}\right)^{1/2}, \quad (9)$$

[1]We note that there is another $R$-parity violating (long-range) diagram for $0\nu\beta\beta$ which depends on $\lambda'_{113}\lambda'_{131}$. This can be tested via $B^0_d$-$\bar{B}^0_d$ mixing [11].

[2]Note that there is a partial cancellation between $\lambda'_{111}$ contributions to atomic parity violation through the up- and down-squarks, leading to somewhat less stringent limits than other experiments.

where in the second expression the limit is obtained, neglecting possible large cancellations between different heavy neutrinos, which would lead to less stringent limits. With this caveat, we see that the upper limit on $\lambda'_{111}$ can be much less stringent than $S_{ei}$, in particular, for masses of $\mathcal{O}(1\ \text{TeV})$, because the dependence on the relevant particle mass is different.

The role that $\lambda'_{111}$ and $S_{ei}$ play in the 4j production is also different. Future $e^-e^-$ colliders will have sufficient energies to produce same-sign $W$ pairs. On the other hand, whether same-sign $\tilde{e}_L$ pairs could be produced on-shell via electroweak interaction depends on the mass of $\tilde{e}_L$. If this is kinematically allowed, this can be followed by LNV decay into jets. For the heavy mass mechanism, the same-sign $W$ production cross section is approximately proportional to $|S^2_{ei}|^2$. The production can then be followed by the decay of the $W$'s into four (first generation) jets with known branching ratios. Using Eq. (9) we see that the same-sign $W$ pair production cross section should be smaller compared with on-shell same-sign $\tilde{e}_L$ production for neutralino/heavy neutrino masses of $\mathcal{O}(1\ \text{TeV})$. For the light mass mechanism, the small $m_{ee}$ value renders the 4j signal unobservable in practice [14,15].

Since the $\lambda'_{111}$ coupling can be of $\mathcal{O}(1)$, the decay of $\tilde{e}_L$ into jets could also be enhanced when compared with the heavy/light mass mechanism. More precisely, the branching ratio $\mathcal{BR}(\tilde{e}_L \to jj)$ depends on the $\lambda'_{111}$ coupling and the presence of competing decay channels, for example, through MSSM gauge interaction $\tilde{e}_L \to e\tilde{\chi}^0$. If the latter channel is open,[3] i.e. when $m_{\tilde{e}_L} > m_{\tilde{\chi}^0} + m_e$, $\mathcal{BR}(\tilde{e}_L \to jj)$ can be suppressed for $m_{\tilde{e}_L}$ and $m_{\tilde{\chi}^0}$ of $\mathcal{O}(100\ \text{GeV})$, but will be much larger for $m_{\tilde{e}_L/\tilde{\chi}^0}$ of $\mathcal{O}(1\ \text{TeV})$ due to the scaling of the $\lambda'_{111}$ coupling; cf. Eq. (8). However, even in the $\mathcal{O}(100\ \text{GeV})$ region, $\mathcal{BR}(\tilde{e}_L \to jj)$ can still be large in the narrow band where $m_{\tilde{e}_L} - m_{\tilde{\chi}^0} \ll m_{\tilde{e}_L}$. If the selectron is the lightest supersymmetric particle, then in the absence of other $R$-parity violating couplings, $\mathcal{BR}(\tilde{e}_L \to jj) = 1$.

Whether $m_{\tilde{\chi}^0} < m_{\tilde{e}_L}$ or $m_{\tilde{\chi}^0} > m_{\tilde{e}_L}$, the mass and total width of $\tilde{e}_L$ can be reconstructed by looking at the dijet invariant mass distributions. Together with the observation of the other $\tilde{e}_L$ decay channels, $\mathcal{BR}(\tilde{e}_L \to jj)$ and hence the value of $\lambda'_{111}$ could be estimated. Furthermore, the mass of $\tilde{\chi}^0$ could be estimated using the rate of the $e^-e^- \to \tilde{e}^-_L\tilde{e}^-_L$ process.

To sum up this section, we have seen qualitatively that for the $\lambda'$MSSM model, there are regions of parameter space where the LNV process $e^-e^- \to 4j$ could be observed, despite the smallness of the closely related $0\nu\beta\beta$ amplitude. We have further argued that the 4j cross section could be much larger than other possible $0\nu\beta\beta$ models, specifically the light and heavy mass mechanisms. The prospects for observing the 4j events also depend on the center-of-mass energy, while an observation could allow inference of the $0\nu\beta\beta$ contribution from the $\tilde{e}_L$ mediated diagrams. In the next section, we shall perform a more quantitative analysis with a simplified $\lambda'$MSSM model, and discuss the prospects for observing 4j events at different center-of-mass energies, sparticle mass regions, as well as with different (future) $0\nu\beta\beta$ limits. Our study will be at the cross section level, while a more detailed analysis, for example, mass reconstruction and precise determination of $\mathcal{BR}(\tilde{e}_L \to jj)$ is beyond the scope of this exploratory study.

## III. FOUR-JET CROSS SECTIONS IN $e^-e^-$ COLLIDERS

In this section, we calculate the total cross section of the 4j signal, $\sigma(e^-e^- \to 4j)$, in a simplified $\lambda'$MSSM model using MADGRAPH5 V1.3.2 [22]. The model is obtained by extending the SM to include the sparticles and vertices involved in the LNV interaction terms derived from Eqs. (6) and (7), in addition to the relevant MSSM QCD and electroweak interactions. For concreteness, we assume that only one neutralino, denoted $\tilde{\chi}^0$, contributes to both $0\nu\beta\beta$ and the 4j process, and that $\tilde{\chi}^0$ is the bino, the superpartner of the $U(1)_Y$ gauge boson. The on-shell $\tilde{e}_L$ pair production cross section $\sigma(e_Le_L \to \tilde{e}_L\tilde{e}_L)$ is given by [23]

$$\sigma(e^-_Le^-_L \to \tilde{e}^-_L\tilde{e}^-_L) = \frac{\pi\alpha^2|g_L|^4}{s}\frac{2m^2_{\tilde{\chi}^0}}{s + 2m^2_{\tilde{\chi}^0} - 2m^2_{\tilde{e}_L}} \times\left[L + \frac{2\lambda}{(s + 2m^2_{\tilde{\chi}^0} - 2m^2_{\tilde{e}_L})^2 - \lambda^2}\right], \tag{10}$$

where

$$L = \ln\frac{s + 2m^2_{\tilde{\chi}^0} - 2m^2_{\tilde{e}_L} + \lambda}{s + 2m^2_{\tilde{\chi}^0} - 2m^2_{\tilde{e}_L} - \lambda}, \qquad \lambda = \lambda(s, m^2_{\tilde{e}_L}, m^2_{\tilde{e}_L}) = \sqrt{s^2 - 4sm^2_{\tilde{e}_L}}, \tag{11}$$

and $g_L$ is the coupling between $e^-_L$, $\tilde{e}^-_L$ and $\tilde{\chi}^0$. The adjustable model parameters are

$$m_{\tilde{\chi}^0}, \quad m_{\tilde{g}}, \quad m_{\tilde{e}_L}, \quad m_{\tilde{u}_L}, \quad m_{\tilde{d}_R}, \quad \lambda'_{111}, \tag{12}$$

while default MADGRAPH values for the SM parameters are used. Specifying these parameters allows the partial widths $\Gamma(\tilde{e}_L \to jj)$, $\Gamma(\tilde{e}_L \to e\tilde{\chi}^0)$ and the corresponding branching ratios $\mathcal{BR}(\tilde{e}_L \to jj)$, $\mathcal{BR}(\tilde{e}_L \to e\tilde{\chi}^0)$ to be computed. The calculation of the 4j cross section uses all contributing diagrams, a subset of which is displayed in Fig. 2. Finite width effects are also included.

The value of $\lambda'_{111}$ is taken assuming two scenarios:

(i) $T_{1/2}(^{76}\text{Ge}) = 1.9 \cdot 10^{25}$ yrs, i.e. $0\nu\beta\beta$ is "just around the corner," [cf. Eq. (1)]; and

[3]For simplicity, we assume all other sparticles to be much heavier than $\tilde{e}_L$.

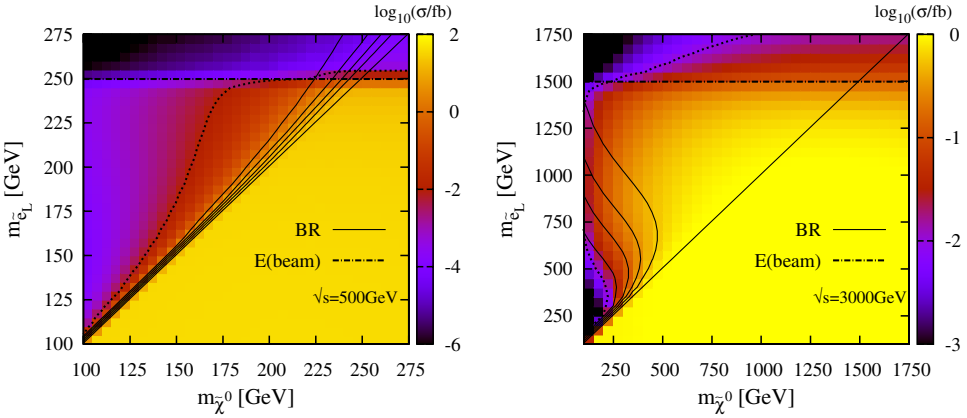


FIG. 3 (color online). Four-jet cross sections (fb) as functions of $(m_{\tilde{\chi}^0}, m_{\tilde{e}_L})$ at 500 GeV (left) and 3 TeV (right) center-of-mass energy, assuming $0\nu\beta\beta$ is dominated by the $\lambda'$MSSM mechanism, and $T_{1/2}(^{76}\mathrm{Ge}) = 1.9 \cdot 10^{25}$ yrs. Here the squark masses are set to 1000 TeV so that their contributions to both $0\nu\beta\beta$ and the 4j cross section are negligible. In both panels, selectrons can be pair-produced on-shell below the dot-dashed line labeled E(beam). The solid lines are branching fractions $\mathcal{BR}(\tilde{e}_L \to jj)$ (from right to left) from 1 to 0.2 in steps of 0.2. In the region to the right of the dotted lines, approximately five or more events might be expected assuming an integrated luminosity of 500 fb$^{-1}$.

(ii) $T_{1/2}(^{76}\mathrm{Ge}) = 1.0 \cdot 10^{27}$ yrs, i.e. expected half-life limit in a ton-scale experiment.

For simplicity, a possible contribution from a $m_{ee}$ term to $0\nu\beta\beta$, which could have a different physical origin, is not included when calculating the $\lambda'_{111}$ upper limit. This is a very valid assumption in case neutrinos would obey a normal hierarchy (as predicted in typical grand unified theories), with $m_{ee} = \mathcal{O}(\mathrm{meV})$. The extraction of $\lambda'_{111}$ follows Ref. [11] (see also Refs. [18–20]), using the nuclear matrix elements in Refs. [19,20].

First we consider the case for $\sqrt{s} = 500$ GeV, which corresponds to the proposed ILC energy [24]. Using the Heidelberg-Moscow $0\nu\beta\beta$ upper limit on $\lambda'_{111}$, the cross section as a function of $(m_{\tilde{\chi}^0}, m_{\tilde{e}_L})$ is displayed in Fig. 3 (left plot). We also show in the figure the region where $\sigma(e^-e^- \to 4j) > 0.01$ fb. In this region, five events or more might be expected assuming an integrated luminosity of 500 fb$^{-1}$ [24]. The squark contributions to both $0\nu\beta\beta$ and the 4j cross sections are decoupled by setting $(m_{\tilde{g}}, m_{\tilde{u}_L}, m_{\tilde{d}_R}) = 1000$ TeV. Other single coupling bounds on $\lambda'_{111}$ are much less stringent than the bound from $0\nu\beta\beta$. In this scenario, the mass of $\tilde{e}_L$ must be smaller than 250 GeV for it to be pair-produced. From Eq. (8), we see that this mass range implies a much smaller value of $\lambda'_{111}$ compared to the hypercharge coupling $g_Y$. As discussed in Sec. II, for $m_{\tilde{e}_L} > m_{\tilde{\chi}^0}$ a large $\mathcal{BR}(\tilde{e}_L \to jj)$ is hence possible only for a narrow band near $m_{\tilde{e}_L} = m_{\tilde{\chi}^0}$. This is reflected in the plot by the correlation between $\sigma(e^-e^- \to 4j)$ and $\mathcal{BR}(\tilde{e}_L \to jj)$, since the four-jet process is well approximated using the narrow width approximation. In this region, $\sigma(e^-e^- \to 4j)$ can be of $\mathcal{O}$(1–10) fb, leading to a good prospect for the observation of the 4j signal. Away from the $m_{\tilde{e}_L} \gtrsim m_{\tilde{\chi}^0}$ band, there is a significant region of parameter space where $\sigma(e^-e^- \to 4j) > \mathcal{O}(0.01)$ fb, which could also lead to a small number of 4j events. When $m_{\tilde{e}_L} < m_{\tilde{\chi}^0}$, $\mathcal{BR}(\tilde{e}_L \to jj) = 1$. In this case, the 4j cross section is of $\mathcal{O}$(10–50) fb and depends relatively mildly on the actual $(m_{\tilde{\chi}^0}, m_{\tilde{e}_L})$ values; see Eq. (10). The cross section falls sharply when $m_{\tilde{e}_L}$ increases beyond the 250 GeV threshold, which is a simple reflection of the narrow $\tilde{e}_L$ width at this mass value.

Next we consider the higher energy option, $\sqrt{s} =$ 3 TeV, the proposed CLIC[4] energy [25]. The cross section as a function of $(m_{\tilde{\chi}^0}, m_{\tilde{e}_L})$ is displayed in Fig. 3 (right plot). Again we assume $T_{1/2}(^{76}\mathrm{Ge}) = 1.9 \cdot 10^{25}$ yrs, and set $(m_{\tilde{g}}, m_{\tilde{u}_L}, m_{\tilde{d}_R}) = 1000$ TeV. We again delineate the region where $\sigma(e^-e^- \to 4j) > 0.01$ fb, which would lead to an expectation of five or more events assuming an integrated luminosity of 500 fb$^{-1}$. We see that the linear collider can access the "natural" $\tilde{e}_L$ and $\tilde{\chi}^0$ mass scale of $\mathcal{O}(1)$ TeV, where the upper $\lambda'_{111}$ limit from $0\nu\beta\beta$ is of $\mathcal{O}(1)$. Now the width $\Gamma(\tilde{e}_L \to jj)$ can dominate over the competitive channel $\Gamma(\tilde{e}_L \to e\tilde{\chi}^0)$ in a much larger region of $(m_{\tilde{e}_L}, m_{\tilde{\chi}^0})$ parameter space. Much of the parameter space where $m_{\tilde{e}_L} > m_{\tilde{\chi}^0}$ has cross sections of $\mathcal{O}(0.1)$ fb or more, leading to $\mathcal{O}(50)$ or more events with an assumed luminosity of 500 fb$^{-1}$. When compared with Eq. (10), which is applicable when $m_{\tilde{e}_L} < m_{\tilde{\chi}^0}$ and when the narrow width approximation is valid, the large $\Gamma(\tilde{e}_L \to jj)$ leads to slightly smaller cross sections. The large width effect that has been included in the calculation can also be seen in the kinematic threshold at $m_{\tilde{e}_L} = 1.5$ TeV, where the cross section drops smoothly as the mass crosses over this limit.

[4]The ILC and the CLIC luminosities are expected to be similar. For ease of comparison the same values are used in the following.

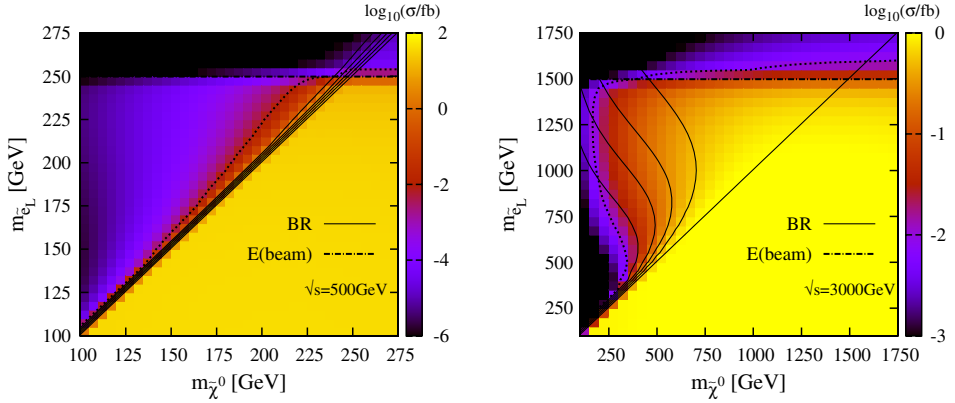


FIG. 4 (color online). Four-jet cross sections (fb) as functions of $(m_{\tilde{\chi}^0}, m_{\tilde{e}_L})$ at 500 GeV (left) and 3 TeV (right) center-of-mass energy, assuming $0\nu\beta\beta$ is dominated by the $\lambda'$MSSM mechanism, and $T_{1/2}(^{76}\mathrm{Ge}) = 1 \cdot 10^{27}$ yrs. Here the squark masses are set to 1000 TeV so that their contributions to both $0\nu\beta\beta$ and the 4j cross section are negligible. In both panels, selectrons can be pair-produced on-shell below the dot-dashed line labeled E(beam). The solid lines are branching fractions $\mathcal{BR}(\tilde{e}_L \to jj)$ (from right to left) from 1 to 0.2 in steps of 0.2. In the region to the right of the dotted lines, approximately five or more events might be expected assuming an integrated luminosity of 500 fb$^{-1}$.

We now consider how the prospect for observing the four-jet events changes when the half-life limit increases to $T_{1/2}(^{76}\mathrm{Ge}) = 1.0 \cdot 10^{27}$ yrs. The cross sections for $\sqrt{s} =$ 500 GeV and $\sqrt{s} = 3$ TeV are shown in the left and right plot of Fig. 4, respectively. Keeping the mass parameters constant, increasing the half-life value leads to a more stringent upper limit on $\lambda'_{111}$. Recall that the same-sign $\tilde{e}_L\tilde{e}_L$ pair is produced via gauge interaction with a $t$-channel neutralino (see the left diagram in Fig. 2). This 2-to-2 process is hence independent of $\lambda'_{111}$, so that this coupling only affects the partial widths and branching ratios of $\tilde{e}_L$. The change in 4j cross section is therefore not proportional to the change in measured $0\nu\beta\beta$ half-life values. This is especially true for the region where we expect the most sensitivity, i.e. $m_{\tilde{e}_L} < m_{\tilde{\chi}^0}$ and $m_{\tilde{e}_L} \gtrsim m_{\tilde{\chi}^0}$, since in these regions the total $\tilde{e}_L$ width is dominated by $\Gamma(\tilde{e}_L \to jj)$. In fact, for $m_{\tilde{e}_L} < m_{\tilde{\chi}^0}$ we have $\Gamma(\tilde{e}_L \to e\tilde{\chi}^0) = 0$, hence $\mathcal{BR}(\tilde{e}_L \to jj) = 1$ and the 4j cross section is independent of $\lambda'_{111}$, up to finite width effects. The value of $\lambda'_{111}$ may be determined by measuring the $\tilde{e}_L$ width.

In the region $m_{\tilde{e}_L} > m_{\tilde{\chi}^0}$, the 4j cross section decreases with $\lambda'_{111}$. The impact of changing $T_{1/2}(^{76}\mathrm{Ge})$ from $1.9 \cdot 10^{25}$ yrs to $1.0 \cdot 10^{27}$ yrs is more pronounced for $\sqrt{s} =$ 500 GeV, as the competing width $\Gamma(\tilde{e}_L \to e\tilde{\chi}^0)$ dominates, and we see that the parameter regions with $\sigma(e^-e^- \to 4j) > 0.01$ fb decreases substantially in the case of $\sqrt{s} =$ 500 GeV. The impact is however somewhat less pronounced for $\sqrt{s} = 3$ TeV, because in most of the parameter space displayed $\mathcal{BR}(\tilde{e}_L \to jj)$ is of $\mathcal{O}(1)$. In this context it might be argued that the 3 TeV CLIC option

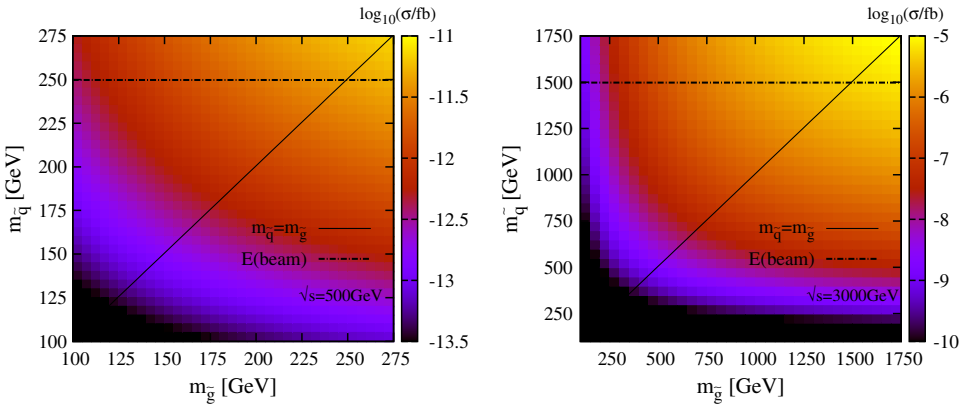


FIG. 5 (color online). Four-jet cross sections (fb) as functions of $(m_{\tilde{g}}, m_{\tilde{q}})$ at 500 GeV (left) and 3 TeV (right) center-of-mass energy, assuming $0\nu\beta\beta$ is dominated by the $\lambda'$MSSM mechanism, and $T_{1/2}(^{76}\mathrm{Ge}) = 1.9 \cdot 10^{25}$ yrs. Here all squark masses are set to a common value $m_{\tilde{q}}$. The slepton and neutralino masses are set to 1000 TeV so that their contributions to both $0\nu\beta\beta$ and the 4j cross section are negligible. The squark mass corresponding to $\sqrt{s}/2$ and the boundary $m_{\tilde{g}} = m_{\tilde{q}}$ are displayed in dot-dashed and solid lines, respectively.

provides a better opportunity to explore the $\lambda'$MSSM $0\nu\beta\beta$ mechanism.

For comparison, we show in Fig. 5 the 4j cross sections obtained if $0\nu\beta\beta$ is dominated by squark-gluino exchanges. Here we assume instead $m_{\tilde{u}_L} = m_{\tilde{d}_R} = m_{\tilde{q}}$, and decouple both $0\nu\beta\beta$ and $\sigma(e^-e^- \to 4j)$ contributions from $\tilde{e}_L$ and $\tilde{\chi}^0$. Again, the $0\nu\beta\beta$ bound is by far the most stringent in this scenario. Since the squarks always appear as $t$-channel propagators, the 4j cross sections are orders of magnitude lower than the $\tilde{e}_L$ dominance scenario. The lack of intermediate particles being produced on-shell also implies that there are no sharp changes in cross sections when the sparticle masses cross over the "kinematic limit" of 250 (1500) GeV in the ILC (CLIC) scenario, nor over the boundary $m_{\tilde{q}} = m_{\tilde{g}}$. Because of the scaling relation Eq. (8), the cross section depends more sensitively on $m_{\tilde{q}}$ than $m_{\tilde{g}}$. Moreover, the cross section ratio of the slepton-neutralino dominance and squark-gluino dominance scenarios decreases when going from $\sqrt{s} = 500$ to $\sqrt{s} = 3000$ GeV. In particular, we see that the cross section is boosted by up to 6 orders of magnitude in the parameter region that we consider, due to the quickly relaxing $\lambda'_{111}$ bound from $0\nu\beta\beta$ when sparticle masses increase. Note that in the $m_{\tilde{q}}$ region around 2 TeV, the $0\nu\beta\beta$ bound is only marginally more stringent than other low energy bounds discussed in Sec. II. The latter can be more stringent when increasing $m_{\tilde{q}}$ beyond 2 TeV.

## IV. SUMMARY AND DISCUSSIONS

Let us briefly comment on the complementarity between the 4j final state and other collider searches. At the LHC, there are signatures that could (indirectly) constrain the $\lambda'$MSSM $0\nu\beta\beta$ mechanism. As discussed in Refs. [10,11], resonant selectron production, followed by the decay chain

$$pp \to \tilde{e}_L \qquad \tilde{e}_L \to e^- \tilde{\chi}^0 \qquad \tilde{\chi}^0 \to e^- jj, \tag{13}$$

leading to same-sign dielectron (SSDE) +jets final states, can be used to test the $\lambda'$MSSM model in the context of $0\nu\beta\beta$. Note that the resonant production process favors large $\lambda'_{111}$, while its gauge decay into an electron favors a small $\lambda'_{111}$. This is different from the 4j signal at lepton colliders, where a large $\lambda'_{111}$ is always preferred. Also, the SSDE signal is only sensitive to the region $m_{\tilde{e}_L} > m_{\tilde{\chi}^0}$. At the cross section level, an excess of SSDE events should be more easily seen when the size of $\lambda'_{111}$ balances these competing effects. At sufficiently low $m_{\tilde{e}_L}$, resonant selectron production becomes suppressed due to the stringent $0\nu\beta\beta$ bound. In addition, the softer electrons and jets would make the search for excess SSDE events more difficult. At sufficiently high $m_{\tilde{e}_L}$, the value of $\lambda'_{111}$ would become large enough that $\mathcal{BR}(\tilde{e}_L \to jj)$ dominates over $\mathcal{BR}(\tilde{e}_L \to e\tilde{\chi}^0)$. It is thus likely that the SSDE channel is most sensitive to some "intermediate" selectron mass region. Additional handles such as cuts on jet multiplicities and missing transverse energies would enhance the signal. The possibility of excluding regions of parameter space using SSDE events from early LHC data is currently under investigation [26].

Note that the ILC is most sensitive to the relatively low mass region $m_{\tilde{e}_L} < 250$ GeV and $m_{\tilde{e}_L} \lesssim m_{\tilde{\chi}^0}$. Because this region is dominated by the $\tilde{e}_L$ decay mode $\tilde{e}_L \to jj$, a resonant selectron produced at the LHC will primarily decay into two jets,

$$pp \to \tilde{e}_L \qquad \tilde{e}_L \to jj, \tag{14}$$

which will likely be overwhelmed by the QCD background given such low $m_{\tilde{e}_L}$. In other words, this region might be best probed by a linear collider. In the very high mass region, the rapidly relaxing $\lambda'_{111}$ would again imply a large dijet resonance cross section at the LHC, while the large decay width could complicate the prospect for (early) detection. Early dijet resonance searches from the ATLAS [27] and CMS [28] Collaborations indicate no significant excess in the dijet invariant mass $m_{jj}$ region ($\sim 800$ GeV $-$ 4 TeV), which may already be able to constrain the parameter region allowed by the current $0\nu\beta\beta$ limit. We postpone a detailed analysis of the impact of dijet exclusion on the $\lambda'$MSSM model in the context of $0\nu\beta\beta$ to a future study. Below $m_{jj} \sim 800$ GeV, the QCD background might overwhelm the signal. However, as can be seen in Figs. 3 and 4, 4j searches at CLIC would be sensitive to a large portion of this region. In any case, since a dijet resonance does not violate lepton number, LNV observables such as the 4j signal will be needed to establish the connection between $0\nu\beta\beta$ and the dijet resonance, should the latter be observed in upcoming LHC data.

Last but not least, note that before running a linear collider in same-sign electron mode, early indication of new physics from $\lambda'$MSSM could already appear in the $e^+e^-$ mode, as opposite-sign $\tilde{e}^+_L \tilde{e}^-_L$ pairs can be produced via a virtual photon or MSSM interactions. If this results in the same 4j signature, it is important to run in the same-sign electron mode to search for lepton number violating effects that can be connected to $0\nu\beta\beta$. The possibility to change the polarization of the electron beams could further allow investigation of the left-handed nature of the 4j process being considered.

To summarize, in this paper we have demonstrated the potential for future linear lepton colliders in providing hints of underlying $0\nu\beta\beta$ mechanisms by looking for four-jet events in same-sign $e^-e^-$ collisions. We have argued that for the $\lambda'$MSSM model, there are good prospects for observing these 4j events, especially when the selectrons can be pair-produced on-shell. However, if $0\nu\beta\beta$ is dominated by squark-gluino exchange, the resulting 4j rate would be too low to be observed. For the former scenario, the properties that the $\lambda'$MSSM model possesses in order to make the 4j cross section larger than that of other $0\nu\beta\beta$ mechanisms, in particular, the light and heavy mass mechanisms, were discussed.

We then went on to compute the 4j cross section for the $\lambda'$MSSM model, assuming $\sqrt{s} = 500$ GeV (ILC) and $\sqrt{s} = 3$ TeV (CLIC) center-of-mass energies. We find that, if the $\tilde{e}_L$ and $\tilde{\chi}^0$ masses are around the 500–1500 GeV region, the 4j signal can be observed at CLIC, while the ILC should also be sensitive to the regions $m_{\tilde{e}_L} \gtrsim m_{\tilde{\chi}^0}$ and $m_{\tilde{e}_L} < m_{\tilde{\chi}^0}$ for $m_{\tilde{e}_L} < 250$ GeV. It is likely that there are regions of parameter space where the LHC could provide indication that $\lambda'$MSSM is relevant for $0\nu\beta\beta$, in which case future linear colliders could act as further and presumably cleaner tests of the $\lambda'$MSSM model. There are other regions which can only be probed by future linear colliders. Further understanding the potentials afforded by the LHC, and its possible synergy with linear colliders on both $\lambda'$MSSM and other $0\nu\beta\beta$ mechanisms, is an interesting topic that should be studied in greater detail in the future.

## ACKNOWLEDGMENTS

We thank Tilman Plehn for a helpful discussion. This work has been supported in part by the Isaac Newton Trust, the STFC, and a Royal Society International Travel Grant (C. H. K.). W. R. was supported by the ERC under the Starting Grant MANITOP and by the Deutsche Forschungsgemeinschaft in the Transregio 27. C. H. K. would like to thank the Particle and Astroparticle Physics group at MPIK Heidelberg and the Rudolf Peierls Centre for Theoretical Physics at Oxford for hospitality while part of the work was carried out.

[1] F. T. Avignone, III, S. R. Elliott, and J. Engel, Rev. Mod. Phys. **80**, 481 (2008).
[2] W. Rodejohann, Int. J. Mod. Phys. E **20**, 1833 (2011).
[3] J. J. Gomez-Cadenas, J. Martin-Albo, M. Mezzetto, F. Monrabal, and M. Sorel, arXiv:1109.5515.
[4] A. Halprin, P. Minkowski, H. Primakoff, and S. P. Rosen, Phys. Rev. D **13**, 2567 (1976); A. Halprin, S. T. Petcov, and S. P. Rosen, Phys. Lett. **125B**, 335 (1983); P. Bamert, C. P. Burgess, and R. N. Mohapatra, Nucl. Phys. **B438**, 3 (1995).
[5] R. N. Mohapatra and J. D. Vergados, Phys. Rev. Lett. **47**, 1713 (1981).
[6] R. N. Mohapatra and G. Senjanovic, Phys. Rev. D **23**, 165 (1981).
[7] M. Hirsch, H. V. Klapdor-Kleingrothaus, and S. G. Kovalenko, Phys. Rev. D **54**, R4207 (1996).
[8] R. N. Mohapatra, Phys. Rev. D **34**, 3457 (1986); J. D. Vergados, Phys. Lett. B **184**, 55 (1987); M. Hirsch, H. V. Klapdor-Kleingrothaus, and S. G. Kovalenko, Phys. Lett. B **352**, 1 (1995); Phys. Rev. Lett. **75**, 17 (1995); K. S. Babu and R. N. Mohapatra, Phys. Rev. Lett. **75**, 2276 (1995); M. Hirsch, H. V. Klapdor-Kleingrothaus, and S. G. Kovalenko, Phys. Lett. B **372**, 181 (1996).
[9] H. V. Klapdor-Kleingrothaus *et al.*, Eur. Phys. J. A **12**, 147 (2001).
[10] B. C. Allanach, C. H. Kom, and H. Päs, Phys. Rev. Lett. **103**, 091801 (2009).
[11] B. C. Allanach, C. H. Kom, and H. Päs, J. High Energy Phys. 10 (2009) 026.
[12] V. Tello, M. Nemevsek, F. Nesti, G. Senjanovic, and F. Vissani, Phys. Rev. Lett. **106**, 151801 (2011).
[13] T. G. Rizzo, Phys. Lett. **116B**, 23 (1982).
[14] G. Belanger, F. Boudjema, D. London, and H. Nadeau, Phys. Rev. D **53**, 6292 (1996).
[15] W. Rodejohann, Phys. Rev. D **81**, 114001 (2010).
[16] M. Hirsch, H. V. Klapdor-Kleingrothaus, S. Kolb, and S. G. Kovalenko, Phys. Rev. D **57**, 2020 (1998); F. Cuypers, G. J. van Oldenborgh, and R. Ruckl, Nucl. Phys. **B409**, 128 (1993); K. Huitu, J. Maalampi, and M. Raidal, Nucl. Phys. **B420**, 449 (1994); C. Blochinger, H. Fraas, G. A. Moortgat-Pick, and W. Porod, Eur. Phys. J. C **24**, 297 (2002); J. L. Feng and M. E. Peskin, Phys. Rev. D **64**, 115002 (2001).
[17] L. E. Ibanez and G. G. Ross, Phys. Lett. B **260**, 291 (1991); L. E. Ibanez and G. G. Ross, Nucl. Phys. **B368**, 3 (1992); T. Banks and M. Dine, Phys. Rev. D **45**, 1424 (1992); H. K. Dreiner, C. Luhn, and M. Thormeier, Phys. Rev. D **73**, 075007 (2006).
[18] M. Hirsch, H. V. Klapdor-Kleingrothaus, and S. G. Kovalenko, Phys. Rev. D **53**, 1329 (1996).
[19] A. Faessler, S. Kovalenko, and F. Simkovic, Phys. Rev. D **58**, 115004 (1998).
[20] A. Faessler and F. Simkovic, J. Phys. G **24**, 2139 (1998).
[21] R. Barbier *et al.*, Phys. Rep. **420**, 1 (2005).
[22] J. Alwall, M. Herquet, F. Maltoni, O. Mattelaer, and T. Stelzer, J. High Energy Phys. 06 (2011) 128; J. Alwall *et al.*, J. High Energy Phys. 09 (2007) 028; F. Maltoni and T. Stelzer, J. High Energy Phys. 02 (2003) 027.
[23] W.-Y. Keung and L. Littenberg, Phys. Rev. D **28**, 1067 (1983).
[24] N. Phinney *et al.*, ILC Reference Design Report, http://www.linearcollider.org/about/publications/reference-design-report.
[25] E. Adli *et al.*, CLIC Conceptual Design Report, http://project-clic-cdr.web.cern.ch/project-CLIC-CDR/.
[26] C. H. Kom *et al.*, (unpublished).
[27] G. Aad *et al.* (ATLAS Collaboration), arXiv:1108.6311; New J. Phys. **13**, 053044 (2011); Phys. Rev. Lett. **105**, 161801 (2010).
[28] S. Chatrchyan *et al.* (CMS Collaboration), Phys. Lett. B **704**, 123 (2011); V. Khachatryan *et al.* (CMS Collaboration), Phys. Rev. Lett. **105**, 211801 (2010).